Allele-specific tumor spectrum in *Pten* knockin mice

Hui Wang[a,b,c], Matt Karikomi[a,b,c,1], Shan Naidu[a,b,c,d,1], Ravi Rajmohan[a,b,c,1], Enrico Caserta[a,b,c], Hui-Zi Chen[a,b,c,e], Maysoon Rawahneh[a,b,c], Julie Moffitt[a,b,c], Julie A. Stephens[f], Soledad A. Fernandez[f], Michael Weinstein[a,b,c], Danxin Wang[g], Wolfgang Sadee[g], Krista La Perle[d], Paul Stromberg[d], Thomas J. Rosol[d], Charis Eng[h], Michael C. Ostrowski[i,j,2], and Gustavo Leone[a,b,c,e,j,2]

[a]Department of Molecular Genetics, College of Biological Sciences, [b]Human Cancer Genetics Program, Comprehensive Cancer Center, College of Medicine, [c]Department of Molecular Virology, Immunology, and Medical Genetics, College of Medicine, [d]Department of Veterinary Biosciences, College of Veterinary Medicine, [e]Medical Scientist Program, College of Medicine, [f]Center for Biostatistics, College of Medicine, [g]Department of Pharmacology, College of Medicine, [i]Department of Molecular and Cellular Biochemistry, College of Medicine, and [j]Tumor Microenvironment Program, Comprehensive Cancer Center, College of Medicine, Ohio State University, Columbus, OH 43210; and [h]Genomic Medicine Institute, Lerner Research Institute and Taussing Cancer Institute, Cleveland Clinic, Cleveland, OH 44195

Edited* by Albert de la Chapelle, Ohio State University Comprehensive Cancer Center, Columbus, OH, and approved January 29, 2010 (received for review November 2, 2009)

Germline mutations in the tumor suppressor gene *PTEN* (phosphatase and tensin homology deleted on chromosome 10) cause Cowden and Bannayan–Riley–Ruvalcaba (BRR) syndromes, two dominantly inherited disorders characterized by mental retardation, multiple hamartomas, and variable cancer risk. Here, we modeled three sentinel mutant alleles of *PTEN* identified in patients with Cowden syndrome and show that the nonsense $Pten^{\Delta 4-5}$ and missense $Pten^{C124R}$ and $Pten^{G129E}$ alleles lacking lipid phosphatase activity cause similar developmental abnormalities but distinct tumor spectra with varying severity and age of onset. Allele-specific differences may be accounted for by loss of function for $Pten^{\Delta 4-5}$, hypomorphic function for $Pten^{C124R}$, and gain of function for $Pten^{G129E}$. These data demonstrate that the variable tumor phenotypes observed in patients with Cowden and BRR syndromes can be attributed to specific mutations in *PTEN* that alter protein function through distinct mechanisms.

cancer genetics | Cowden syndrome

The tumor suppressor gene *PTEN* (phosphatase and tensin homology deleted on chromosome ten) encodes a product with both protein and lipid phosphatase activity (1–3). The lipid phosphatase activity negatively regulates phosphoinositide-3 kinase (PI-3K) and the downstream Akt and mammalian target of rapamycin pathway components (4). Consistent with a requirement for lipid phosphatase activity in tumor suppression, the mutant $PTEN^{G129E}$ allele, originally identified in patients with Cowden syndrome, selectively lacks lipid phosphatase activity (5). However, PTEN also has protein phosphatase activity, and although controversial, there is a body of evidence suggesting that PTEN's protein phosphatase activity may also contribute to tumor suppression (6). The Cowden syndrome $PTEN^{C124R}$ allele, which encodes a protein product lacking lipid and protein phosphatase activity (7), provides genetic support for an involvement of dual PTEN phosphatase activities in tumor suppression. In addition, recent data suggest a role for nuclear PTEN in genomic stability that may be independent of its lipid phosphatase and PI-3K signaling activities (8). Despite intensive efforts in the past decade to understand the biochemical functions of PTEN, it remains unclear which of its many functions endow this gene with tumor suppressor status and whether the different functions contribute to tumor suppression selectively in an organ-specific and/or signaling pathway-specific manner.

Individuals with Cowden syndrome show a wide variation in disease manifestation, including cancer predisposition (9), that is thought to be driven by a combination of genotype as well as polymorphic heterogeneity in the population (10). The reason why polymorphic heterogeneity has been invoked is because identical mutations result in disparate phenotypes, ranging from mild developmental disorders in Cowden syndrome to very severe disorders in Bannayan–Riley–Ruvalcaba (BRR) syndrome (9). Here, we used homologous recombination in mice to model three different mutant alleles of *PTEN* originally identified in Cowden syndrome. We found that each mutant allele displayed distinct tumor phenotypes in organs targeted by Cowden syndrome. These functional differences are not manifested during embryonic development and do not correspond strictly to the level of Akt activation. Rather, the variable phenotypes can be attributed to functions beyond PI3K-Akt activation that include gain of function for the $Pten^{G129E}$ allele and loss of function for the $Pten^{\Delta 4-5}$ and $Pten^{C124R}$ alleles. Together, these results demonstrate that specific germline mutations have a strong influence in the variable predisposition to cancer of patients who have Cowden syndrome.

Results

Abnormal Embryonic Development in $Pten^{\Delta 4-5}$, $Pten^{G129E}$, and $Pten^{C124R}$ Knockin Mice. To explore the physiological consequence of inactivating distinct arms of PTEN's tumor suppressor arsenal, we generated, characterized, and compared mouse models that have a frameshift ($Pten^{\Delta 4-5}$) (11) leading to the premature stop and missense mutations in *Pten* ($Pten^{G129E}$ or $Pten^{C124R}$) that can be found in patients with Cowden syndrome (12) (Fig.1*A*). Targeting of the three *Pten* mutant alleles was verified by Southern blot analysis, PCR, and direct sequencing of genomic DNA (11) (Fig.1 *B* and *C* and Fig. S1*A*, *Left*). Allelic expression imbalance analysis showed that the two missense mutant alleles lacking the neomycin (neo) cassette (neo−) were expressed at a similar level as the WT allele (Fig.1*D*), whereas the same mutant alleles containing the neo cassette (neo+) were expressed, as expected, at lower levels (Fig.S1*A*, *Right*).

We first evaluated the effect of $Pten^{\Delta 4-5}$, $Pten^{G129E}$, and $Pten^{C124R}$ on embryonic development by examining offspring derived from intercrosses between heterozygous knockin mice (Fig. 2*A*). The intercrosses yielded no live homozygous progeny at birth for any of the three mutant alleles; however, mutant embryos were recovered at embryo day (E) 8.5 and E9.5, albeit at a lower than expected frequency. Development of the few mutant embryos that were obtained was severely compromised, with defects in anterior-posterior patterning, failure of axial rotation, and absence of overt tissue differentiation leading to resorption by E9.5 (Fig. 2 *A* and *B* and Fig. S1*B*). Heterozygous $Pten^{\Delta 4-5/+}$,

Author contributions: H.W., M.C.O., and G.L. designed research; H.W., M.K., S.N., R.R., E.C., H.-Z.C., M.R., and J.M. performed research; D.W. and W.S. contributed new reagents/analytic tools; H.W., H.-Z.C., J.A.S., S.A.F., M.W., D.W., W.S., K.L.P., P.S., T.J.R., C.E., M.C.O., and G.L. analyzed data; and H.W., M.C.O., and G.L. wrote the paper.

The authors declare no conflict of interest.

*This Direct Submission article had a prearranged editor.

[1]M.K., S.N., and R.R. contributed equally to this work.

[2]To whom correspondence may be addressed. E-mail: michael.ostrowski@osumc.edu or gustavo.leone@osumc.edu.

This article contains supporting information online at www.pnas.org/cgi/content/full/0912524107/DCSupplemental.

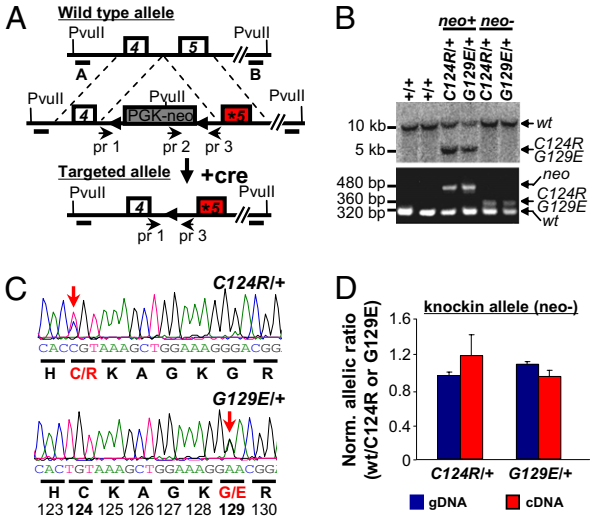

Fig. 1. Generation, targeting, and verification of point mutations of *Pten* alleles. (*A*) Endogenous WT *Pten* allele (*Top*), the two targeted missense mutations in *exon 5* (*) of *Pten* allele containing the selectable phosphoglycerate kinase promoter (PGK)-neo cassette (flanked by *Lox*P sites, triangles; *Middle*), and the two targeted mutant *Pten* knockin alleles ($Pten^{C124R}$ and $Pten^{G129E}$) lacking the PGK-neo cassette (after mating with *EIIA-cre*-expressing mice; *Bottom*). A and B, DNA probes used for Southern blot analysis; pr, primers used for PCR genotyping. (*B*) Southern blot analysis (*Upper*) and genotyping PCR (*Lower*) of tail DNA with the indicated genotypes. Genomic DNA was digested with PvuII and probed with probe A, and expected band sizes are indicated for each allele. PCR amplification using primer pairs 1–3 and 2–3 (primer information provided in Table S3) yielded specific fragment size for different alleles as indicated. (*C*) Sequence analysis of tail DNA isolated from $Pten^{C124R/+}$ and $Pten^{G129E/+}$ mice. Chromatograms demonstrating the successful targeting of the *Pten* locus and translated amino acids are shown below the codons. Red letters and bold numbers denote the two targeted amino acids (*C124R* and *G129E*). Arrows point to targeted nucleotides. (*D*) Allelic expression imbalance analysis of allele-specific expression. The graph shows the proportion of mRNA expressed from the WT allele over the indicated mutant allele in lungs of $Pten^{C124R/+}$ and $Pten^{G129E/+}$ mice. neo−, mice lacking the PGK-neo cassette. Genomic DNA (gDNA) was used as an internal control.

$Pten^{G129E/+}$, and $Pten^{C124R/+}$ embryos were morphologically indistinguishable from WT littermates (Fig. 2 *A* and *B* and Fig. S1*C*). Thus, overall, there were no obvious differences among homozygous knockin embryos of the three *Pten* mutant genotypes.

Organ-Selective Cancer Predisposition in $Pten^{\Delta 4-5/+}$, $Pten^{G129E/+}$, and $Pten^{C124R/+}$ Mice. The tumor spectrum in animals harboring one copy of each of the three mutant *Pten* alleles was determined by analyzing groups of >40 adult male and female mice. Similar to previous studies that analyzed heterozygous mice harboring a *Pten* knockout allele (13–17), mice carrying one copy of each of the three *Pten* mutant alleles exhibited neoplasms in multiple organs that are characteristically involved in patients who have Cowden syndrome, confirming these are causal mutations that drive this syndrome. Interestingly, pathological examination of 9-month-old mice revealed differences in the frequency and severity of the individual proliferative lesions found in the three genetic groups (Table S1). The intergroup differences were amplified when the propensity of an individual animal to develop tumors at two or more organ sites was considered (Fig. 2*C*). A significant bias for lesions also occurred in specific organ pairs for each of the three genetic cohorts. Mammary gland-lymph node ($P < 0.001$), uterus-lymph node ($P = 0.032$), thyroid-lymph node ($P = 0.003$), and prostate-stomach ($P = 0.003$) lesions were frequently present in $Pten^{\Delta 4-5/+}$ mice; mammary gland-lymph node ($P = 0.050$) lesions were present in $Pten^{G129E/+}$ mice;

A

Table 1. Embryo viability

		+/+	m/+	m/m	Total
E9.5					
C124R	observed	**19**	**37**	0(14)*	**70**
	expected	*18*	*35*	*18*	
G129E	observed	**8**	**35**	0(3)*	**46**
	expected	*12*	*24*	*12*	
Δ4-5	observed	**6**	**16**	0(3)*	**25**
	expected	*6*	*13*	*6*	
E8.5		**+/+**	***m/+***	***m/m***	**Total**
C124R	observed	**14**	**46**	0(11)*	**71**
	expected	*18*	*36*	*18*	
G129E	observed	**20**	**43**	0(3)*	**66**
	expected	*17*	*33*	*17*	
Δ4-5	observed	**14**	**45**	0(6)*	**65**
	expected	*16*	*33*	*16*	

*p < 0.001, Chi-square test or Fisher's exact test

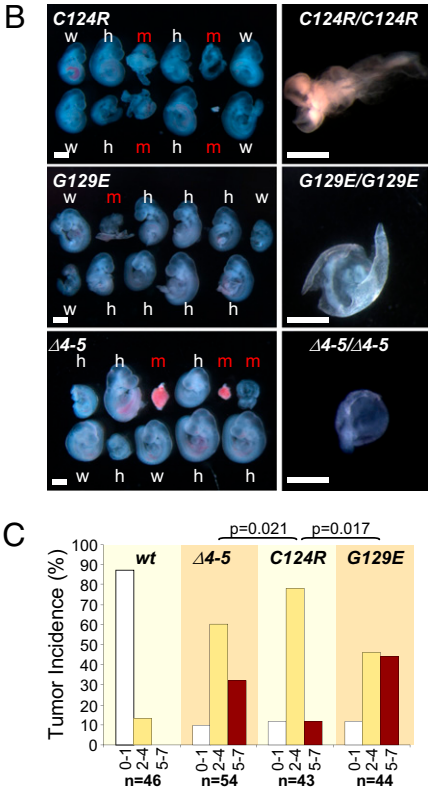

Fig. 2. $Pten^{\Delta 4-5}$, $Pten^{C124R}$, and $Pten^{G129E}$ mutations cause early embryonic lethality and exhibit allele-specific tumor syndromes. (*A*) Offspring from *Pten* ($Pten^{C124R}$, $Pten^{G129E}$, or $Pten^{\Delta 4-5}$) heterozygous intercrosses were examined. The number of observed and expected E8.5 and E9.5 embryos is indicated. Fisher's exact or χ^2 tests were used to compare differences between observed and expected homozygous embryos. The number of dead embryos is shown in parentheses. *m*, mutant allele ($Pten^{C124R}$, $Pten^{G129E}$, or $Pten^{\Delta 4-5}$). (*B*) (*Left*) Stereomicroscopic images of E9.5 WT (w), heterozygous (h), and homozygous (m) *Pten*-mutant littermate embryos. (*Right*) Higher magnification images of severely affected homozygous mutant embryos. (Scale bar: 1 mm.) (*C*) Organ distribution of tumor lesions in animals harboring the indicated *Pten* alleles. To simplify the graphical representation of data, mice were grouped based on the number of organs (0–1, white bars; 2–4, yellow bars; 5–7, red bars) afflicted with tumors. All uncategorized data were analyzed by Poisson regression methods, and significant differences are shown; all *Pten* mutant-WT allele comparisons were significant ($P < 0.0001$; not indicated).

and mammary gland-intestine ($P = 0.007$), mammary gland-adrenal ($P = 0.049$), and prostate-stomach ($P = 0.002$) lesions were present in $Pten^{C124R/+}$ mice (Table S2). Consistent with observations made in human patients with Cowden syndrome, there was a gender bias in the organ-specific manifestation of lesions, with lymph node lesions

more frequently found in female mice (for $Pten^{\Delta 4-5}$, $P < 0.001$) and adrenal and stomach lesions more commonly found in male mice (for $Pten^{\Delta 4-5}$, $P = 0.008$ and $P = 0.012$, respectively; for $Pten^{C124R}$, $P = 0.034$) (Fig. S2). These findings challenge the current view of polymorphic heterogeneity in the population as the principal reason for the variable penetrance observed in patients with Cowden syndrome. We suggest that this variability may instead be attributed, at least in part, to allele-specific effects of *PTEN* mutations.

Based on these initial observations, we performed a thorough histopathological analysis of neoplastic lesions in organ sites frequently involved in Cowden syndrome, including the uterus, thyroid, mammary gland (2, 18–20) and the prostate (21). Detailed

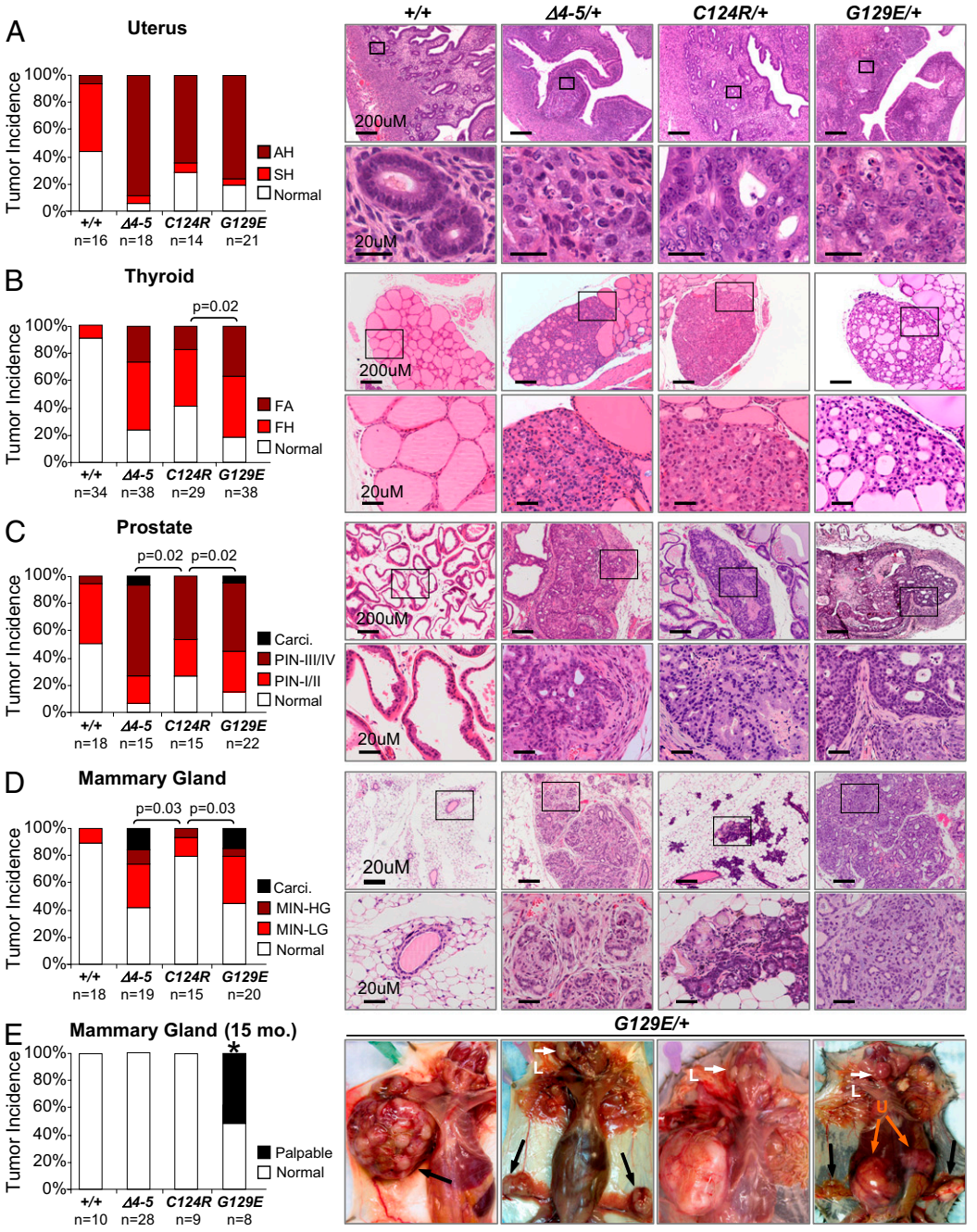

Fig. 3. Allele-specific and organ-specific tumor development in $Pten^{\Delta 4-5/+}$, $Pten^{C124R/+}$, and $Pten^{G129E/+}$ mice. Histopathological grades of lesions were compared between WT, $Pten^{\Delta 4-5/+}$, $Pten^{C124R/+}$, and $Pten^{G129E/+}$ 9-month-old mice in the uterus (*A*), thyroid (*B*), prostate (*C*), and mammary gland (*D*). Note the significant difference in the severity of lesions among the various animals with mutant *Pten* alleles. (*Right*) Histology with the highest grade lesions found in each genetic group. (*Lower*) Magnified view of the boxed region in the upper panels. Detailed histopathological criteria used to grade the lesions are included in Fig. S3. AH, atypical hyperplasia; SH, simple hyperplasia; PIN-I/II, prostatic intraepithelial neoplasia grade I or II; PIN-III/IV, prostatic intraepithelial neoplasia grade III or IV; FA, follicular adenoma; FH, follicular hyperplasia; Carci., carcinoma; MIN, mammary intraepithelial neoplasia; LG, low grade; HG, high grade; Normal, no gross or microscopic tumor. Comparisons between genetic groups in *A–D* were analyzed by χ^2 or Fisher's exact tests and adjusted by Holm's method. (*E*) Large palpable tumor masses in 12–15-month-old $Pten^{G129E/+}$ female mice. Black and orange arrows point to mammary gland and uterine (U) tumors, respectively. White arrows point to enlarged lymph nodes (L). Normal, no gross mammary gland tumors; Palpable, palpable mammary gland tumors. Comparisons between genetic groups in *E* were analyzed by a binomial exact test. All comparisons between $Pten^{G129E/+}$ and other genetic groups were found to be significant (*$P < 0.01$).

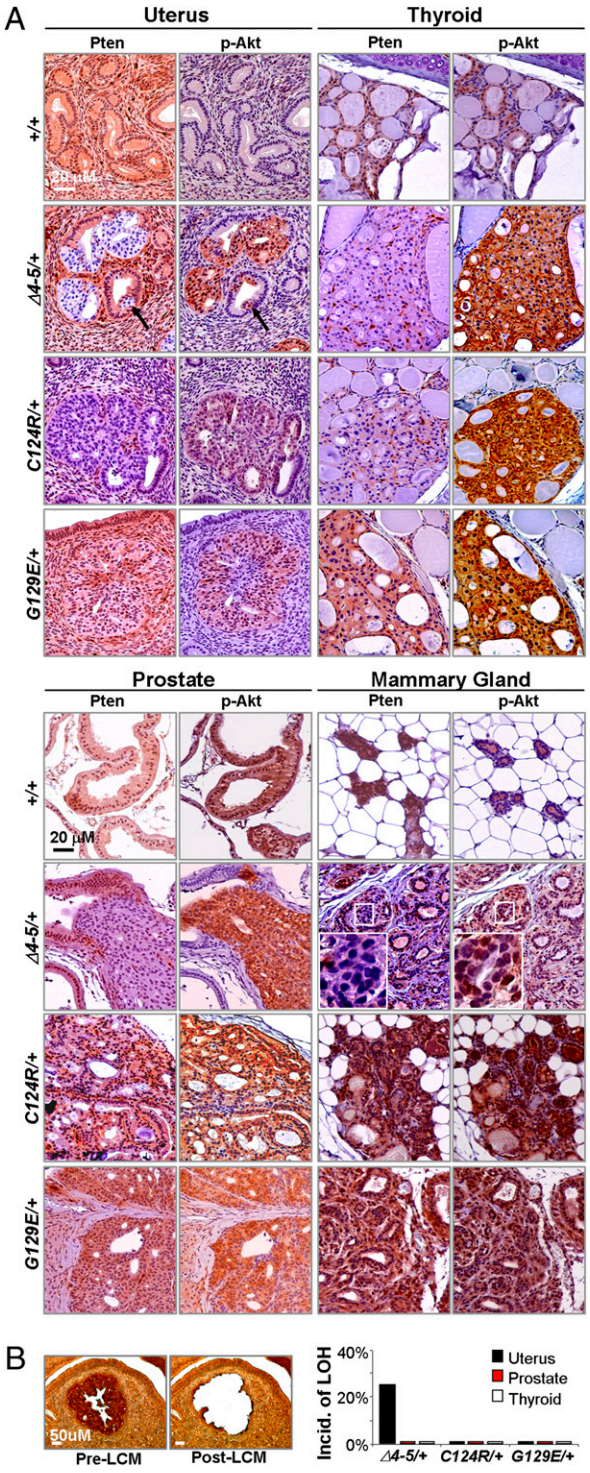

Fig. 4. Expression of Pten and p-Akt in proliferative lesions of various organs. (*A*) Tissue sections from the uterus and thyroid (*Upper*) or prostate and mammary gland (*Lower*) of mice with the indicated genotypes were stained with Pten- and p-Akt-specific antibodies. Complete loss of Pten occurred in $Pten^{\Delta 4-5/+}$ lesions of the uterus, thyroid, and prostate, whereas decreased levels of Pten were observed in $Pten^{C124R/+}$ lesions of the uterus and thyroid. Pten protein expression was lost in a mosaic fashion in advanced lesions of $Pten^{\Delta 4-5/+}$ mice but persisted in $Pten^{C124R/+}$ MIN and $Pten^{G129E/+}$ mammary gland carcinomas. (*Right*) Magnified images of the boxed region. (*B*) LOH analysis of WT *Pten* allele detected by PCR from laser capture microdissected (LCM) lesions of the uterus, prostate, and thyroid of 9-month-old heterozygotes. (*Left*) Representative images showing pre- and post-LCM tissue of "quick" p-Akt immunostained sections. (*Right*) Incidence of LOH in lesions from the indicated organs. For LOH in the uterus, 25 $Pten^{\Delta 4-5/+}$, 5 $Pten^{C124R/+}$, and 5 $Pten^{G129E/+}$ mice were examined. LOH in other organs was sampled from 5 mice per genotype group.

criteria for grading lesions are presented in Fig. S3. In the uterus, proliferative lesions of the endometrium (simple hyperplasia and atypical hyperplasia) were encountered in $Pten^{\Delta 4-5/+}$, $Pten^{C124R/+}$, and $Pten^{G129E/+}$ female mice with equal frequency (Fig. 3*A*), similar to what has been reported in patients with Cowden syndrome. Advanced thyroid follicular lesions, however, were more frequently observed in $Pten^{G129E/+}$ mice compared with $Pten^{\Delta 4-5/+}$ or $Pten^{C124R/+}$ mice (Fig. 3*B* and Fig. S4*A*). In the prostate, both $Pten^{\Delta 4-5/+}$ and $Pten^{G129E/+}$ mice were more likely to have lesions of higher histological grade, which included prostatic adenocarcinoma, than $Pten^{C124R/+}$ mice (Fig. 3*C*). In the mammary gland, advanced lesions such as mammary intraepithelial neoplasia (MIN), invasive carcinoma, and adenosquamous carcinoma were observed in both $Pten^{\Delta 4-5/+}$ and $Pten^{G129E/+}$ female mice but rarely in $Pten^{C124R/+}$ female mice (Fig. 3*D*; $P = 0.03$). Strikingly, only lesions in $Pten^{G129E/+}$ female mice ($n = 8$) advanced to form large palpable tumors with unique adenosquamous morphology and a prominent stromal component (Fig. 3*E* and Fig. S4*B*), which are classic characteristics of breast carcinoma seen in individuals with Cowden syndrome (22). Despite small sample sizes in our database comprising >400 *PTEN* mutation-positive individuals, all three $PTEN^{G129E}$-affected women had breast cancer, whereas two $PTEN^{C124R}$-affected individuals only had fibrocystic disease of the breast. Moreover, we also observed high-grade MIN in $Pten^{G129E/+}$ male mice but not in males of other genotypes (Fig. S4*C*), consistent with an increased incidence of breast cancer observed in male patients with Cowden syndrome with this particular *PTEN* mutation (5, 23). The development of more severe lesions in select organs of $Pten^{G129E/+}$ mice when compared with $Pten^{\Delta 4-5/+}$ mice suggests that the $Pten^{G129E}$ allele, in addition to lacking lipid phosphatase activity, may have gained protumorigenic functions. Together, these findings demonstrate the critical role of specific *PTEN* mutant alleles in driving the broad clinical manifestations of Cowden syndrome that often present in an organ-selective fashion and with variable penetrance and expressivity.

Organ-Specific *Pten* Inactivation During Tumor Initiation and Progression. Molecular analysis of embryos and tumors with each of the three different *Pten* mutant genotypes revealed intriguing tissue-specific mechanisms of how *Pten* mutant alleles differentially contribute to tumor development and progression. As might have been expected, there was focal loss of WT Pten protein expression in $Pten^{\Delta 4-5/+}$ epithelial lesions of the endometrium, thyroid, and prostate (Fig. 4*A*). In the endometrial lesions analyzed, there was loss of heterozygosity (LOH) in 25% of cases (Fig. 4*B*). In the remaining endometrial lesions, as well as in the limited number of thyroid and prostate $Pten^{\Delta 4-5/+}$ tumors analyzed, LOH was not observed (Fig. 4*B*), consistent with the low percentage of LOH (11%) observed in Cowden syndrome-related nonmalignant neoplasias (24). These results suggest that the frequency of LOH in neoplastic lesions of all three mutant heterozygotes was low and that loss of expression from the WT *Pten* allele in the majority of $Pten^{\Delta 4-5/+}$ tumors was mediated by a posttranscriptional mechanism.

Interestingly, Pten protein in lesions of the uterus, thyroid, and prostate was frequently absent in hyperplastic clonal areas containing as few as three to five cells (Fig. 4*A* and Fig. S5 *A–C*), suggesting that loss of Pten expression in these organs was an early or initiating event during tumor development. In mammary preneoplastic lesions, however, $Pten^{\Delta 4-5/+}$ female mice retained normal amounts of Pten protein, and its loss, which was manifested

in a mosaic pattern, was only detected in advanced adenocarcinomas (Fig. 4*A* and Fig. S5*D*). When we examined epithelial cells from three adenocarcinomas in $Pten^{\Delta 4-5/+}$ and $Pten^{G129E/+}$ female mice, no LOH was detected in any of these samples. From these data, we conclude that the level of WT Pten protein that accumulates in $Pten^{\Delta 4-5/+}$ mammary glands is haploinsufficent to suppress tumor initiation, and that loss of expression from the WT allele is a late event that may be required for malignant progression of mammary cancers. Together, these observations support a tissue-selective requirement for loss of Pten protein expression.

Allele-Specific Mechanism of Pten-Mediated Tumor Suppression. Inactivation of tumor suppression by the two missense mutations ($Pten^{G129E}$ and $Pten^{C124R}$) is thought to result from the ablation of enzymatic phosphatase activity (1, 25, 26). It was therefore surprising to find that lesions in the uterus, thyroid, and prostate of $Pten^{C124R/+}$ mice had little (if any) detectable Pten protein (Fig. 4*A*). This was specific to this cohort of mice, because Pten protein in the corresponding lesions of $Pten^{G129E/+}$ mice was clearly present. Interestingly, the levels of Pten protein in preneoplastic mammary gland lesions in $Pten^{C124R/+}$ mice were uniformly high, suggesting that, as in $Pten^{\Delta 4-5/+}$ mice, tumor initiation in mammary glands did not require LOH (note that carcinoma was never detected in this genetic group) (Fig. 4*A*). These results suggest that the two missense mutations ($Pten^{G129E}$ and $Pten^{C124R}$) contribute to tumorigenesis differently, with the $Pten^{C124R}$ allele producing a protein product that is particularly labile.

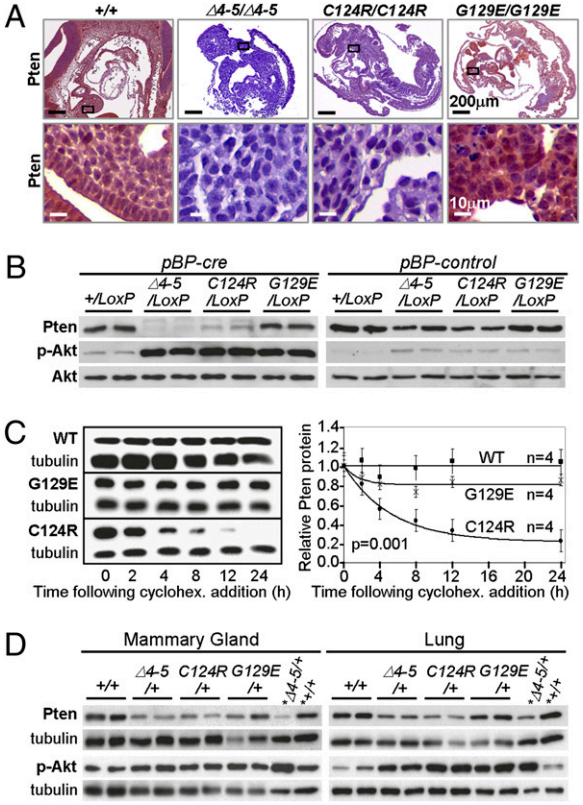

Fig. 5. Decreased $Pten^{C124R}$ protein stability. (*A*) Pten IHC staining of homozygous embryos (E9.5) with the indicated genotypes. (*Lower*) High magnification of boxed areas in the upper panels. (*B*) Western blots of control- (*pBP-control*) or *cre*-retrovirus- (*pBP-cre*) infected MEFs of the indicated genotypes were probed with antibodies specific for Pten, p-Akt S473, and total Akt. Complete *cre*-mediated deletion of exons 4 and 5 was confirmed by PCR (Fig. S6*B*). (*C*) (*Left*) Western blots of cycloheximide- (cyclohex.) treated MEFs treated as in *B* and expressing WT Pten (WT), $Pten^{C124R}$ (C124R), and $Pten^{G129E}$ (G129E). (*Right*) Protein half-lives of WT Pten (WT), $Pten^{C124R}$ (C124R), and $Pten^{G129E}$ (G129E) were calculated as described in *SI Text* and plotted. n, number of independent experiments. ANOVA with a repeated-measures model was used to evaluate differences across the various time points and between genotypes. (*D*) Western blots of lysates derived from mammary glands and lungs of two 9-month-old female mice with the indicated genotypes probed with Pten- and p-Akt (S473)-specific antibodies as indicated. *Lysates derived from MEFs with the indicated genotypes were included in these blots. Tubulin protein levels were monitored as a loading control.

The unexpectedly low levels of $Pten^{C124R}$ protein in tumors prompted us to reexamine its expression in normal tissues. We used immunohistochemistry (IHC) to compare Pten protein levels in E9.5 $Pten^{+/+}$, $Pten^{\Delta 4-5/\Delta 4-5}$, $Pten^{G129E/G129E}$, and $Pten^{C124R/C124R}$ embryos. Remarkably, $Pten^{C124R}$ protein was almost undetectable in most tissues of homozygous embryos (Fig. 5*A*), even though its mRNA levels were not altered. In contrast, there were normal amounts of Pten protein expressed from the $Pten^{G129E}$ allele. To determine whether the absence of $Pten^{C124R}$ protein could be attributable to reduced protein stability, we generated and compared mouse embryonic fibroblasts (MEFs) containing a conditional $Pten^{LoxP}$ null allele (with *LoxP* sites flanking exons 4–5) and either a WT allele or each of the three mutant knockin alleles ($Pten^{+/LoxP}$, $Pten^{\Delta 4-5/LoxP}$, $Pten^{G129E/LoxP}$, and $Pten^{C124R/LoxP}$; Fig. S6*A*). Retroviral transduction of cre recombinase (*cre*) in the MEF cultures resulted in efficient deletion of $Pten^{LoxP}$ (Fig. S6*B*), generating cells that express *Pten* solely from the remaining WT allele or from each of the three knockin alleles (Fig. S6*B*). Western blot analysis confirmed normal steady-state levels of Pten protein in *cre-*$Pten^{+/LoxP}$ and *cre-*$Pten^{G129E/LoxP}$ MEFs (compared with *control-*$Pten^{\Delta 4-5/LoxP}$ MEFs), undetectable Pten in *cre-*$Pten^{\Delta 4-5/LoxP}$ MEFs, and decreased Pten in *cre-*$Pten^{C124R/LoxP}$ MEFs (Fig. 5*B*). Quantitative RT-PCR analysis showed equivalent amounts of *Pten* mRNA in MEFs of all genotypes (Fig. S6*C*). Pulse-chase experiments using cycloheximide demonstrated a significant reduction in the half-life of $Pten^{C124R}$ protein when compared with either WT or $Pten^{G129E}$ protein ($P = 0.001$; ~3.7 vs. >24 h; Fig. 5*C*). From these results, we suggest that one mechanism by which the $Pten^{C124R}$ allele promotes Cowden syndrome and sporadic cancers is through the inherent instability of its protein product.

The activation of Akt, through its PI-3K-mediated phosphorylation at either residue 308 or 473, is thought to be attributable to the inactivation of Pten (1). Indeed, the level of phosphorylated Akt (p-Akt) was increased in *cre-*$Pten^{\Delta 4-5/LoxP}$ MEFs relative to either *cre-*$Pten^{+/LoxP}$ or *control-*$Pten^{\Delta 4-5/LoxP}$ MEFs. Interestingly, p-Akt levels were similarly increased in MEFs expressing $Pten^{G129E}$ or $Pten^{C124R}$ protein (Fig. 5*B*). Moreover, IHC revealed that E9.5 $Pten^{\Delta 4-5/\Delta 4-5}$, $Pten^{G129E/G129E}$, and $Pten^{C124R/C124R}$ embryos had equivalent levels of p-Akt, indicating that signaling downstream of PI-3K in embryos of all three mutant genotypes was similarly engaged (Fig. S1*B*). Because $Pten^{\Delta 4-5/+}$, $Pten^{G129E/+}$, and $Pten^{C124R/+}$ mice had different tumor and gender biases characteristic of Cowden syndrome with distinct pathological findings and frequencies, we investigated the extent of Akt phosphorylation in tumor samples. Again, IHC of all tumor types and Western blot analysis of lysates derived from mammary glands, lungs, and MEFs failed to reveal any difference in the amounts of p-Akt between the three genotypes (Figs. 4*A* and 5 *B* and *D*). Therefore, the severity of cancer phenotypes attributed to $Pten^{C124R}$, $Pten^{G129E}$, and $Pten^{\Delta 4-5}$ alleles did not correspond to Akt activation (8, 27, 28). These data indicate that unique functions, beyond Akt activation, distinguish the three mutant alleles from one another in their ability to instigate cancer development and progression.

Discussion

Germline *PTEN* mutations cause a broad array of seemingly unrelated syndromes, which are collectively called the PTEN hamartoma tumor syndrome and include BRR and Cowden syndromes (9). Puzzlingly, certain identical mutations, such as

R130× and R233×, can result in either Cowden or BRR syndrome (29), suggesting that polymorphic heterogeneity strongly influences disease outcome. Even individuals with Cowden syndrome have a wide variation in disease manifestation and in the penetrance of phenotypes, including cancer predisposition (2, 12, 30). Whether this variability is attributable to gene mutations that differentially alter the function of Pten protein directly or to polymorphic variation and/or mutations in genetic modifiers of *PTEN* has been a subject of controversy (16).

Mouse modeling of three important mutant alleles of *PTEN* identified in patients with Cowden syndrome demonstrates that nonsense ($Pten^{\Delta 4-5}$) and missense ($Pten^{G129E}$ and $Pten^{C124R}$) mutations in *Pten* display distinct tumor phenotypes in organs targeted by Cowden syndrome. These functional differences are not manifested during embryonic development and do not appear to depend on differential PI-3K-Akt signaling. We have not formally ruled out, however, the possibility that the timing of Akt activation during tumor initiation/progression may differ between the three *Pten* knockin genetic groups. Nonetheless, it is interesting that phenotypic differences in human patients with Cowden syndrome also do not strictly correspond to the level of Akt activation. Rather, the striking differences in tumor spectrum and severity, with phenotypes in $Pten^{G129E/+} > Pten^{\Delta 4-5/+} >> Pten^{C124R/+}$ mice, may be partially accounted for by a gain of function in $Pten^{G129E/+}$ individuals and by reduced protein stability in $Pten^{C124R/+}$ individuals. The gain-of-function phenotypes manifested in $Pten^{G129E/+}$ mice may be attributable to the remaining protein phosphatase activity of mutant protein or to interference of function by mutant protein in protein complexes. Although further experimentation will be required to define fully the mechanisms underlying our observations, the in vivo models we describe provide the physiological and genetic foundation necessary to unravel this puzzle. In summary, the results demonstrate that specific germline mutations disrupt PTEN function by distinct mechanisms that may explain the organ-selective variability associated with cancer predisposition in Cowden syndrome. These findings raise the possibility that specific somatic alterations, whether genetic or epigenetic, in *PTEN* will also have a differential impact on sporadic cancers that develop in patients who do not have Cowden syndrome. We believe that the genotype-phenotype relations revealed here may be used to guide more effective and personalized targeted therapies for cancer patients with *PTEN* mutations.

Methods

$Pten^{C124R/+}$ and $Pten^{G129E/+}$ knockin mice were generated using a standard homologous recombination approach. Isolation of primary MEFs from E13.5 embryos, retroviral infections, and cell culture conditions were done using standard methods. $Pten^{LoxP}$ deletion by *cre* was confirmed by genotyping of MEF DNA and Western blot analysis using PTEN antibody. Statistics analyses were performed for all the data. Detailed methods can be found in *SI Text*.

ACKNOWLEDGMENTS. The authors thank John C. Thompson for excellent technical assistance, the Ohio State University Comprehensive Cancer Center Nucleic Acids and Transgenics Shared Facilities for technical assistance, and Dr. Philip Popovich and Wenmin Lai for guidance in the laser capture microdissection technique. This work was funded by National Institutes of Health Grants R01CA85619, R01HD47470, and P01CA097189 (to G.L.) and R01CA053271 and P01CA097189 (to M.C.O.). H.W. is supported by an American Cancer Society Postdoctoral Fellowship. M.C.O received awards from both the Susan Komen Foundation and the Evelyn Simmers Foundation, and G.L. received an award from the Susan Komen Foundation and US Department of Defense. G.L. is the recipient of the Pew Charitable Trusts Scholar Award and the Leukemia and Lymphoma Society Scholar Award.

1. Maehama T, Dixon JE (1998) The tumor suppressor, PTEN/MMAC1, dephosphorylates the lipid second messenger, phosphatidylinositol 3,4,5-trisphosphate. *J Biol Chem* 273: 13375–13378.
2. Li J, et al. (1997) PTEN, a putative protein tyrosine phosphatase gene mutated in human brain, breast, and prostate cancer. *Science* 275:1943–1947.
3. Myers MP, et al. (1997) P-TEN, the tumor suppressor from human chromosome 10q23, is a dual-specificity phosphatase. *Proc Natl Acad Sci USA* 94:9052–9057.
4. Manning BD, Cantley LC (2007) AKT/PKB signaling: Navigating downstream. *Cell* 129: 1261–1274.
5. Liaw D, et al. (1997) Germline mutations of the PTEN gene in Cowden disease, an inherited breast and thyroid cancer syndrome. *Nat Genet* 16:64–67.
6. Leslie NR, Maccario H, Spinelli L, Davidson L (2009) The significance of PTEN's protein phosphatase activity. *Adv Enzyme Regul* 49:190–196.
7. Nelen MR, et al. (1997) Germline mutations in the PTEN/MMAC1 gene in patients with Cowden disease. *Hum Mol Genet* 6:1383–1387.
8. Shen WH, et al. (2007) Essential role for nuclear PTEN in maintaining chromosomal integrity. *Cell* 128:157–170.
9. Gustafson S, Zbuk KM, Scacheri C, Eng C (2007) Cowden syndrome. *Semin Oncol* 34: 428–434.
10. Pezzolesi MG, Platzer P, Waite KA, Eng C (2008) Differential expression of PTEN-targeting microRNAs miR-19a and miR-21 in Cowden syndrome. *Am J Hum Genet* 82: 1141–1149.
11. Trimboli AJ, et al. (2009) Pten in stromal fibroblasts suppresses mammary epithelial tumours. *Nature* 461:1084–1091.
12. Marsh DJ, et al. (1999) PTEN mutation spectrum and genotype-phenotype correlations in Bannayan-Riley-Ruvalcaba syndrome suggest a single entity with Cowden syndrome. *Hum Mol Genet* 8:1461–1472.
13. Suzuki A, et al. (1998) High cancer susceptibility and embryonic lethality associated with mutation of the PTEN tumor suppressor gene in mice. *Curr Biol* 8:1169–1178.
14. Di Cristofano A, Pesce B, Cordon-Cardo C, Pandolfi PP (1998) Pten is essential for embryonic development and tumour suppression. *Nat Genet* 19:348–355.
15. Podsypanina K, et al. (1999) Mutation of Pten/Mmac1 in mice causes neoplasia in multiple organ systems. *Proc Natl Acad Sci USA* 96:1563–1568.
16. Freeman D, et al. (2006) Genetic background controls tumor development in PTEN-deficient mice. *Cancer Res* 66:6492–6496.
17. Stambolic V, et al. (2000) High incidence of breast and endometrial neoplasia resembling human Cowden syndrome in pten+/– mice. *Cancer Res* 60:3605–3611.
18. Risinger JI, Hayes AK, Berchuck A, Barrett JC (1997) PTEN/MMAC1 mutations in endometrial cancers. *Cancer Res* 57:4736–4738.
19. Dahia PL, et al. (1997) Somatic deletions and mutations in the Cowden disease gene, PTEN, in sporadic thyroid tumors. *Cancer Res* 57:4710–4713.
20. Steck PA, et al. (1997) Identification of a candidate tumour suppressor gene, MMAC1, at chromosome 10q23.3 that is mutated in multiple advanced cancers. *Nat Genet* 15: 356–362.
21. Cairns P, et al. (1997) Frequent inactivation of PTEN/MMAC1 in primary prostate cancer. *Cancer Res* 57:4997–5000.
22. Schrager CA, Schneider D, Gruener AC, Tsou HC, Peacocke M (1998) Clinical and pathological features of breast disease in Cowden's syndrome: An underrecognized syndrome with an increased risk of breast cancer. *Hum Pathol* 29:47–53.
23. Fackenthal JD, et al. (2001) Male breast cancer in Cowden syndrome patients with germline PTEN mutations. *J Med Genet* 38:159–164.
24. Marsh DJ, et al. (1998) Germline PTEN mutations in Cowden syndrome-like families. *J Med Genet* 35:881–885.
25. Myers MP, et al. (1998) The lipid phosphatase activity of PTEN is critical for its tumor suppressor function. *Proc Natl Acad Sci USA* 95:13513–13518.
26. Ramaswamy S, et al. (1999) Regulation of G1 progression by the PTEN tumor suppressor protein is linked to inhibition of the phosphatidylinositol 3-kinase/Akt pathway. *Proc Natl Acad Sci USA* 96:2110–2115.
27. Vivanco I, et al. (2007) Identification of the JNK signaling pathway as a functional target of the tumor suppressor PTEN. *Cancer Cell* 11:555–569.
28. Chang CJ, et al. (2008) PTEN nuclear localization is regulated by oxidative stress and mediates p53-dependent tumor suppression. *Mol Cell Biol* 28:3281–3289.
29. Eng C (2003) PTEN: One gene, many syndromes. *Hum Mutat* 22:183–198.
30. Eng C, Peacocke M (1998) PTEN and inherited hamartoma-cancer syndromes. *Nat Genet* 19:223.